Published by :
http://www.ijert.org

International Journal of Engineering Research & Technology (IJERT)
ISSN: 2278-0181
Vol. 8 Issue 11, November-2019

A Comparative Analysis of Foundations using Prescriptive Design and Static Loading Test Methods

(Case Study: The Karuma Interconnection Power Project in Uganda)

*Acidri Samuel[1], Kyakula Michael[2], and Mugume Rodgers Bangi[3]
[1, 2, 3] Faculty of Engineering, Department of Civil and Building Engineering, Kyambogo University, Uganda
*Corresponding Author,

***Abstract*: Despite recent improvements in soil characterisation, geotechnical exploration and construction methodologies, 66.7% of overhead transmission line foundation design engineers use prescriptive design methods with applied traditional factors of safety between 2.5 to over 4.0, to design foundations in the face of uncertainties in ground conditions and design criteria, non-linear nature of the load-displacement response of foundations and the prescriptive design's tendency to give linear solutions. Hence, the use of full-scale foundations and static load tests to assess the overall response of foundations. A Ø900mm pile and 3 pad foundations along Uganda's 400 kV Karuma Interconnection Project were designed, constructed and tested under uplift, compression and lateral loads as per the respective failure modes. The results suggested that the maximum displacements were within 0.36-18.96% of the prescriptive 25 mm value for uplift, 3.32% of the prescriptive 25 mm value for compression, and 4.78% of the prescriptive 50 mm value for the lateral load test in conformity to IEC 61773 (1996) and COMESA/FDHS 293 (2007).**

The foundations' insitu load capacities from the hyperbolic graphs as per the Chin-Kondner extrapolation (1971), confirmed that the foundations could adequately resist the working loads at 100% and ultimate design loads at 130%, despite uncertainties of moderately aggressive chemical environment exposures as per BS EN 206 (2013) or soils with medium to high degrees of plasticity with low swell potentials.

Keywords: Foundations, Prescriptive Design, Static Load Tests (SLTs), Transmission Towers

1. INTRODUCTION

1.1 The Local Geology

The geology of Karuma Interconnection Project mainly consists of quaternary rock systems of laterite, alluvium, swamp and lacustrine deposits, Neoproterozoic rock systems of mudstones, shales, slates and phyllites, Mesoproterozoic rock system of mica schists, and Neoarchaean rock systems of metagabbro, porphyritic-granite, meta-dolerite, granodiorite, biotite-hornblende and banded gneiss.

1.2 The Research Background

Foundation substructures are essential structural members that transmit and distribute different kinds of superstructure loads to the substrata below without exceeding the bearing capacity of the ground and preventing excessive or uneven settlements, and they are generally classified as shallow or spread and deep foundations [1-3]. Foundations must fulfil both structural and geotechnical parameters, but due to uncertainties of the subsoil behaviour, most foundations are either statically or dynamically tested to verify conformity with the design load, but the latter is not commonly used in Southern Africa [4,5].

In Uganda, since 2013, load tests have been used to either prove the maximum capacity of the foundation and/or to verify the predicted design values and settlements under pressure on a foundation that is expendable to the main works; and at times on a working pile whilst limiting the maximum test load to less than 1.5 times the safe working load [5-7].

Foundation design entails that neither the foundation units collapse nor should they induce the overall shear failure of the supporting ground, lest the foundation's post-construction settlement values exceed the permissible tolerances in the codes and specifications [8-11]. The design of foundations consists of proportioning the foundation, mitigating limit state conditions such as the ultimate limit state properties of loss of static equilibrium of the structure, failure by collapse or by fatigue; and/or the serviceability limit state properties of deflection, cracking, vibration, and deterioration of the foundation structure [3,12-14].

Uncertainties in geotechnical models and parameters and their effect have long been recognised [15-23]; and hence, to perform geotechnical and foundation designs using the prescriptive design approaches, conservative values of the uncertain soil parameters are often adopted along with an 'experience-calibrated' factor of safety [11, 24]. In the quest to obtain a more rational design, many researchers such as Wu [25], Christian [26], Whitman [18], Phoon [27,28], Fenton [29], Najjar and Gilbert [30], Wang [31], and Zhang [32] have turned to reliability-based designs such as foundation full-scale models, analyses and foundation tests, which creates a much more-realistic geotechnical and foundation design outcome and is better in quantifying the uncertainties in soil parameters than the prescriptive design approaches [24]. Therefore, since also soils can soften or harden upon shearing and have a much more complex response than perfect plasticity; the recent focus on using the realistic full-scale foundation models, provides important insights into the overall response of foundations [33-38].

International Journal of Engineering Research & Technology (IJERT)
ISSN: 2278-0181
Vol. 8 Issue 11, November-2019

2. GEOTECHNICAL INVESTIGATIONS

2.1 The Test Trial Pits and Borehole pits

Four test pits were carefully located at a 1m distance from the survey mark stones, and manually excavated to 1m x 0.5m x 3m dimensions for investigating the stratification of subsurface layers and ground water as per BS 5930: 1999+A2: 2010 and BS 6031: 2009. Obtained soil samples were labelled and placed in air-tight plastic bags for indicative laboratory soil tests.

2.2 The Dynamic Penetration Light Test

The DPL test was used in the determination of the soil's insitu resistance to the dynamic penetration of a cone, and in determining the soil's bearing capacity (q) and resistance values using the Dutch formula below. Thus, the N_{10} values were interpreted to give the respective granular and fine-grained soil consistencies as per BS EN ISO 22476-2: 2005 + A1: 2011 and DIN 4094: 1990.

$$q = q_d = r_d\left[\frac{M}{(M+P)}\right] = \left[\frac{\mathrm{E}}{\mathrm{A \times H}}\right] \times \left[\frac{\mathrm{M}}{(\mathrm{M+P})}\right] \quad (1)$$

$$\mathrm{r_d} = \frac{\mathrm{Mgh}}{\mathrm{A\,e}} = \left[\frac{Mgh \times N_{10}}{0.1A}\right] = \frac{E}{A \times H} \quad (2)$$

Where:
q = soil's bearing capacity/dynamic point resistance
r_d = soil's unit point resistance; and E = Mgh
A = cone area (A = 0.001m^2); H = penetration depth
M = mass of hammer (M = 10.252 kg)
P = total assembly mass where the DPL assembly mass is 6.714 kg, and each rod is 2.86 kg
N_{10} = blows per 10 cm penetration
e = penetration rate = $0.1/N_{10}$

2.3 The Standard Penetration Test

The SPT test was conducted in accordance with BS EN ISO 22476-3:2005 and ASTM D1586-99: 1999 to compute allowable bearing capacities from the corrected SPT $\mathrm{N'_{55}}$ values using the Terzaghi's formula (1967) and Bowles's (1982) approach based on Meyerhof's (1963) equations. The Terzaghi's (1967) formulae is given below:

$$\mathrm{N'_{55}} = \mathrm{C_N \times N \times \eta_1 \times \eta_2 \times \eta_3 \times \eta_4} \quad (3)$$

$$\mathrm{C_N} = \left(\frac{\mathrm{p''_o}}{\mathrm{p'_o}}\right)^{\frac{1}{2}} \text{ for } 0.4 \leq \mathrm{C_N} \leq 1.7 \quad (4)$$

$$\mathrm{q_{ult}} = 5.14 \times \frac{\mathrm{q_u}}{2} = \left[\frac{5.14 \times 13.1 \times \mathrm{N'_{55}}}{2}\right] \quad (5)$$

$$\mathrm{q_{all}} = \frac{\mathrm{q_{ult}}}{\mathrm{FS}} = \frac{5.14 \times \mathrm{c_u}}{\mathrm{FS}} = \left\{\frac{5.14 \times 13.1 \times \mathrm{N'_{55}}}{2 \times \mathrm{FS}}\right\} \quad (6)$$

Where:
$\mathrm{q_{all}}$ = allowable bearing capacity
$\mathrm{C_N}$ = adjustments for overburden pressure
$\mathrm{p'_o}$ = overburden pressure
$\mathrm{p''_o}$ = reference overburden pressure (95.76 kPa)
N = corrected SPT $\mathrm{N'_{55}}$ values
$\eta_1 = \mathrm{E_r/E_{rb}}$ (hammer efficiency correction)
$\mathrm{E_r}$ = average energy ratio
$\mathrm{E_{rb}}$ = standard energy ratio
η_2 = rod length correction
η_3 = sampler correction
η_4 = borehole diameter correction
FOS = factor of safety

Bowles's (1982) approach based on Meyerhof's (1963) equations is given below:

$$\mathrm{q_{all}} = \left\{\frac{\mathrm{N}}{\mathrm{F_2}}\left[\frac{(\mathrm{B+F_3})}{\mathrm{B}}\right]^2 x\, \mathrm{K_d}\right\} \text{for B} > \mathrm{F_4} \quad (7)$$

$$\mathrm{q_{all}} = \left[\frac{\mathrm{N}}{\mathrm{F_1}} x\, \mathrm{K_d}\right] \text{for B} \leq \mathrm{F_4} \quad (8)$$

$$\mathrm{K_d} = \left[1 + \frac{0.33\mathrm{D}}{\mathrm{B}}\right] \leq 1.33 \quad (9)$$

Where:
$\mathrm{q_{all}}$ = allowable bearing capacity
N = corrected SPT $\mathrm{N'_{55}}$ values
$\mathrm{N'_{55}}$ = adjusted N-values
B = foundation width/breadth
$\mathrm{F_1} = 0.05$; $\mathrm{F_2} = 0.08$; $\mathrm{F_3} = 0.3$; and $\mathrm{F_4} = 1.2$
D = foundation depth

Meyerhof's (1963) equations are given below:

$$\mathrm{q_a} = 0.73\,\mathrm{N''}\,\mathrm{R_{D_1}} \times \mathrm{S_a}\ (\mathrm{B} \leq 1.2\mathrm{m}) \quad (10)$$

$$\mathrm{q_a} = 0.48\,\mathrm{N''}\,\mathrm{R_{D_2}}\left(\frac{\mathrm{B}+0.3}{\mathrm{B}}\right)^2 \mathrm{S_a}\ (\mathrm{B} > 1.2\mathrm{m}) \quad (11)$$

$$\mathrm{R_{D_1}} = 1 + 0.2\left(\frac{\mathrm{D_f}}{\mathrm{B}}\right) \leq 1.2 \text{ for } \emptyset = 0 \quad (12)$$

$$\mathrm{R_{D_2}} = 1 + 0.1\left(\frac{\mathrm{D_f}}{\mathrm{B}}\right) \leq 1.2 \text{ for } \emptyset = 0 \quad (13)$$

Where:
$\mathrm{q_a} = \mathrm{q_{all}}$ = allowable bearing capacity
$\mathrm{N''}$ = corrected SPT $\mathrm{N'_{55}}$ values
$\mathrm{R_{D_1}}$ and $\mathrm{R_{D_2}}$ = Meyerhof's depth reduction factors
$\emptyset$ = Internal angle of soil friction in degrees
B = foundation width/breadth (in metres)
$\mathrm{D_f}$ = foundation depth
S_a = Allowable settlement limit of 25 mm

2.4 Indicator Laboratory Soil Tests

The obtained disturbed and undisturbed soil samples were tested for moisture content [39], particle size distribution [40,41], liquid limit [42], plastic limit and plasticity index [43], linear shrinkage limit [43], pH [44,45], sulphate and chloride content [44,46], bulk density and unit weight [43,47], specific gravity [43,48], direct shear [49] and one-dimensional consolidation [50,51].

2.5 Static Load Foundation Tests

Static Load Tests are the most reliable and fundamental forms of in-situ loading tests, considered as the bench-mark of foundation performance and used for validating load capacities and design assumptions of the foundation regarding the axial compression or tension resistance, or its deflected shape under a lateral load. They involve the measurement of foundation head displacements in response to a physically applied test load until its failure point to replicate the long-term sustained load conditions [5,6,52]. They are standardised by ASTM D1143 for static axial compressive test; ASTM D3689 for static axial tensile (or uplift) test, and ASTM D3966 for lateral load test [6,53-56].

2.5.1 The Static Axial Tensile Load Test

As standardised by ASTM D3689/D3689M-07 (2013) and IEC 61773 (1996), the Static Axial Tensile load test was used for verifying the behaviour of vertical or batter tension foundations like those of overhead transmission lines with respect to their tensile capacity and axial stiffness, so as to provide the most reliable relationship between the static tensile load applied axially to a foundation and the resulting axial movements. Hence, the obtained information was used in assessing the foundation shaft's side shear resistance distribution, amount of end-bearing developed and the long-term load-deflection behaviour. It was also used to determine if the foundation had an ultimate static capacity and a deflection at service load satisfactory to support the specified foundation or superstructure [53,57].

2.5.2 The Static Axial Compressive Load Test

The Static Axial Compressive load test measured the axial deflections of vertical or inclined foundations when loaded in static axial compression in order to confirm the foundation's structural and geotechnical reliability and to predict its settlement rate. The load is thus, increased in stages until the proposed working load and a certain factor of safety is reached, and then unloading the load until the rise or rebound has substantially ceased. The foundation may be tested in three cycles, whereby the first cycle is to 150% of foundation's Design Load (DL), the second cycle test is to 200% of DL and the third cycle tests the foundation to its ultimate load, defined as 250% to 300% of its DL [53,54]. Since the procedure leading up to 300% of the Design Load is very time consuming, the commonest method used stops at the first cycle and is limited to between 100% to 130% of the design load [5,6,57].

2.5.3 The Lateral Load Test

As per ASTM D3966/D3966M-07 (2013), the Lateral load test was conducted to measure the lateral deflection of a vertical or inclined foundation when subjected to lateral loading, with the results used in characterising the variation of pile-soil interaction properties such as the coefficient of horizontal subgrade reaction, and estimation of bending stresses and lateral deflection over the pile's length for use in its structural design [53,56].

3. RESULTS AND DISCUSSIONS

3.1 The Test Trial Pits and Borehole pits

Ground water tables were encountered above the base of footings in the swampy locations of KL 30 and AP 104/5 at 0.3m and 1.14m levels respectively; and ground water tables were encountered below the base of footings in locations AP 108/15 and AP 108/20 at levels of below 10m and 4m respectively below existing ground level [58]. The ground water table results in Table 1, were used in computing the soil's effective unit weight (γ'), unit surcharge magnitude (q) and corrections for water table effects on bearing capacities. Also, the insitu soil profile descriptions were used as a precursor assessment to the final soil grading and classifications as shown in Table 2 below.

$$q = \gamma(D_f - D) + \gamma' D \quad (14)$$
$$q = \gamma \mathrm{D_f} \quad (15)$$
$$q = \gamma_{av} \mathrm{D_f} \quad (16)$$

Where:
γ = unit weight; and γ' = effective unit weight
$\gamma_{av} = \frac{1}{B}[\gamma D + \gamma'(B - D)]$ for $(D \le B)$
$\gamma_{av} = \gamma$ for $(D > B)$

Table 1: The insitu ground water table levels

Site	Depth (m)	Pits	WT (m)	FFL (m)
1 (PS)	10.0	BHP	10.0	2.75
2 (GS)	3.0	TP	4.0	3.50
3 (WL)	10.0	BHP	1.14	4.50
4 (PL)	20.0	BHP	0.30	12.8

Note:
1 = AP 108/15; 2 = AP 108/20; 3 = KL 30; 4 = AP 104/5;
PS = Poor Soil; GS = Good Soil; WL = Waterlogged Location;
PL = Pile Location; WT = Water Table; FFL = Foundation's Formation Level; BHP = Borehole Pit; TP = Trial Pit

Table 2: The insitu soil strata descriptions

Site	Depth (m)	Insitu soil strata	Soil Classification
1 (PS)	2.45-4.2	Grey-dense clayey sand	Silty sand (SM)
2 (GS)	0.1-3.5	Brownish-orange laterite* with duricrust	Clayey sand with gravel (SC)
3 (WL)	4.5-6.5	Moist reddish brown, mottled grey, hard gravelly-clays	Gravelly clays of intermediate plasticity (CI)
4 (PL)	12.7-15	Slightly moist greyish brown, medium-dense clayey sand	Clayey sand (SC)

Note:
1 = AP 108/15; 2 = AP 108/20; 3 = KL 30; 4 = AP 104/5;
PS = Poor Soil; GS = Good Soil; WL = Waterlogged Location;
PL = Pile Location

- *Medium-dense gravelly-sand
- SC and SM = Using the USCS soil classification system
- CI = Using the BS 5930 classification system

3.2 The Dynamic Penetration Light (DPL)

The DPL's N_{10} readings of 10 to 54 under the respective penetration rates (e), corresponded to granular soils of medium-dense consistency mainly coarse-grained sandy soils as shown in Tables 3 and 4 below [59,60]. DPL tests were done to determine the blows per 10cm penetrations (N_{10}), consistency descriptions, computations of unit point (r_d) resistance, and dynamic point (q_d) resistance/soil bearing capacity as per Eq. (1) and (2).

Table 3: The DPL result summary for AP 108/20

Depth (m)	$\mathbf{M_1}$ (kg)	$\boldsymbol{N_{10}}$	e (m/blow)	$\boldsymbol{r_d}$ (MPa)	$\boldsymbol{q_d}$ (MPa)
1.0	10.252	10	0.010	4.90	2.7
2.0	10.252	54	0.002	26.46	13.2
3.0	10.252	13	0.008	6.37	2.9
3.5	10.252	14	0.007	6.86	2.9

International Journal of Engineering Research & Technology (IJERT)
ISSN: 2278-0181
Vol. 8 Issue 11, November-2019

Note:
M_1 = mass of hammer; N_{10} = blows per 10 cm penetration
e = penetration rate (m per blow); r_d = unit point resistance
q_d = dynamic point resistance/soil bearing capacity

Table 4: Granular-soil consistency from DPL test

Blows, N_{10}	Consistency description	Blows, N_{10}	Consistency description
Less than 1	Very Loose	7 - 83	Medium Dense
1 - 7	Loose	Over 83	Dense

Source: Nilsson (2012)

3.3 The Standard Penetration Testing

The SPT N-value of fine-grained soils at KL 30 of 100, corresponded to a hard soil consistency, whereas the SPT N-values of coarse-grained soils at locations AP 108/15 and AP 104/5 were 24 and 27 respectively, corresponding to medium-dense soil consistencies as shown in Tables 5 to 7. The SPT results were used in determining the soil's preliminary consistency descriptions using the N-values and parameters for bearing capacity analysis [58,61] as shown in Eq. (3) to (13).

Table 5: The insitu SPT result summaries

Site	SPT N-value	Corrected N_{55}	Soil consistency	Soil Classification
1 (PS)	24	19	Medium-dense	Silty Sand (SM)
3 (WL)	100	77	Hard	Gravelly clays of intermediate plasticity (CI)
4 (PL)	27	20	Medium-dense	Clayey Sand (SC)

Note:
1 = AP 108/15; 2 = AP 108/20; 3 = KL 30; 4 = AP 104/5;
PS = Poor Soil; GS = Good Soil; WL = Waterlogged; PL = Pile

- SC and SM = USCS soil classification system
- CI = BS 5930 soil classification system

Table 6: Consistency table for coarse-grained soils

S/No	Consistency Description	SPT N-values
1	Very Loose	Less than 4
2	Loose	4 to 10
3	Medium-Dense / Compact	10 to 30
4	Dense	30 to 50
5	Very Dense	Over 50

Source: BS 5930: 1999 + A2: 2010

Table 7: Consistency table for fine-grained soils

Description	Unconfined Compressive Strength (kPa)	SPT N-value
Very soft	Less than 25	Less than 2
Soft	25 to 50	2 to 5
Firm	50 to 100	5 to 10
Stiff	100 to 200	10 to 20
Very stiff	200 to 380	20 to 40
Hard	Over 380	Over 40

Source: BS 5930: 1999 + A2: 2010

3.4 The Soil Resistivity Testing

The resistivity values showed that the soils at locations KL 30, AP 108/20 and AP 104/5 were essentially non-corrosive, whereas the soil at AP 108/15 was highly corrosive as shown in Tables 8 and 9 below. The soil resistivity test was used as a preliminary and non-conclusive test to provide generalised insitu environmental exposure conditions which may lead to steel depassivation and corrosion, and affect the structural design of the reinforced concrete foundations. Thus, for a more conclusive study, chemical tests in section 3.11, were deemed necessary regardless of the level of corrosiveness encountered [61,62].

Table 8: The insitu soil resistivity test results

Site	Average soil resistivity (**Ωm**)	Soil corrosiveness description (*See Table 9 below*)
1 (PS)	29.845	Highly corrosive
2 (GS)	1201.472	Essentially non-corrosive
3 (WL)	220.5	Essentially non-corrosive
4 (PL)	285.192	Essentially non-corrosive

Table 9: Resistivity explanations

S/No	Soil Resistivity (Ωm)	Soil Corrosiveness
1	Greater than 200	Essentially non-corrosive
2	100-200	Mildly corrosive
3	50-100	Moderately corrosive
4	30-50	Corrosive
5	10-30	Highly corrosive
6	Less than 10	Extremely corrosive

Source: Roberge (2000)

3.5 The Vane Shear Testing

No vane shear tests (VST) were conducted in the borehole pits as the clay soils encountered were of a 'stiff to very stiff consistency' and not fitting the criteria for tests as per the requirements of ASTM D2573/D2573M-18 (2018). The VST method is not applicable for unsaturated or non-plastic silts, sands, gravels or other high permeability soils which dilate, collapse and generate pore pressures [58,61,63,64].

3.6 The Specific Gravity Testing

The specific gravity (G_s) values showed that the soils at location AP 108/15 were sand with silty particles, AP 108/20 had gravelly soil with clay mineral compositions, KL 30 had clay with gravel particles, and AP 104/5 had sand with clay compositions as shown in Tables 10 and 11. These descriptions are fairly comparable but inconclusive to the final descriptions by the USCS and BS 5930 soil classification systems as discussed in section 3.9. Thus, higher G_s values give higher load bearing capacities since an increase in G_s increases the soil's shear strength parameters and its suitability as a construction material [65-67].

Table 10: Insitu specific gravity summaries

Site	Gs (Mg/m^3)	Generalised soil type	Soil Classifications [USCS & BS 5390]
1 (PS)	2.370 to 2.777	Sand with silty particles	Silty sand (SM)
2 (GS)	2.380 to 2.483	Gravelly soil with clay mineral compositions	Clayey sand with gravel (SC)
3 (WL)	2.453 to 2.739	Clay with gravel particles	Gravelly clays of intermediate plasticity (CI)
4 (PL)	2.640 to 2.73	Sand with clay composition	Clayey sand (SC)

Note:
1 = AP 108/15; 2 = AP 108/20; 3 = KL 30; 4 = AP 104/5;
PS = Poor Soil; GS = Good Soil; WL = Waterlogged; PL = Pile
- SC and SM = Unified Soil Classification System (USCS)
- CI = BS 5930 classification system

Table 11: Specific gravities of some soils

S/No	Type of Soil	Specific gravity (Gs) range (Mg/m^3)
1	Gravel	2.65 - 2.68
2	Quartz Sands	2.64 - 2.66
3	Silty	2.67 - 2.73
4	Clay	2.70 - 2.90
5	Chalk	2.60 - 2.75
6	Loess	2.65 - 2.73
7	Peat / Organic soils	1.30 - 1.90 (Less than 2.0)
	Clay soil mineral compositions	
8	K-Feldspars (1)	2.54 - 2.57
9	Montmorillonite (2)	2.35 - 2.70
10	Illite (2)	2.6 - 3.0
11	Kaolinite (2)	2.6 - 2.68
12	Biotite (1)	2.8 - 3.2

References:
(1) Lambe and Whitman, 1969; (2) Mitchell, 1993
Source: Das (2016); Das and Sobhan (2018)

3.7 The Direct Shear Testing

The direct shear test showed that the friction angle (ϕ) value was greater than that of cohesion (c) ($i.e\ \phi > \emptyset$) at 5.2m depth, and friction angle (ϕ) was less than cohesion (c) ($i.e\ \phi < \emptyset$) at 10.4m depth, despite both soil strata being classified as clayey-sand soils. This showed an increased clay and silt composition in the bottom soil strata since they induce the sand with increased interlocking behaviour/cohesion [63,68]. The obtained results of cohesion (c) and angle of internal friction (ϕ) were used in computing the soil's bearing capacities, pile skin and end-bearing resistances using the lateral earth pressure coefficient. Equations (17) to (19) are bearing capacity formulae for Terzaghi, and Meyerhof's vertical and inclined loads respectively whereas Eq. (20) and (21), and Eq. (22) and (23) are for predominantly clay and sandy soils respectively.

$$q_u = cN_cS_c + 0.5\gamma_t BN_\gamma S_\gamma + \gamma_t D_f N_q \qquad (17)$$
$$q_u = cN_cS_cd_c + q_oN_qS_qd_q + 0.5\gamma BN_\gamma S_\gamma d_\gamma \qquad (18)$$
$$q_u = cN_cd_ci_c + q_oN_qd_qi_q + 0.5\gamma BN_\gamma d_\gamma i_\gamma \qquad (19)$$

$$f_s = \alpha S_u = \alpha\left(\frac{q_u}{2}\right) = \alpha\left(\frac{12 \text{ x } N_{55}}{2}\right) \qquad (20)$$
$$q_b = N_c S_u \omega = \left[N_c\left(\frac{12 \text{ x } N_{55}}{2}\right)\omega\right] \qquad (21)$$
$$f_s = K\bar{q}\tan\delta = [1 - (\bar{q}\sin\emptyset' \, x \tan\emptyset')] \qquad (22)$$
$$q_b = N_q\bar{q} \qquad (23)$$

Where:
f_s = shaft skin resistance; and α = Adhesion factor
S_u = average undrained shear strength
q_u = unconfined compressive strength
q_b = end bearing resistance; and δ = friction angle
N_c, N_q & N_γ = Terzaghi's bearing capacity factors
$\bar{q}$ = effective overburden pressures
$\emptyset'$ = effective internal friction angle from SPT test
K = lateral earth pressure coefficient

Table 12: Insitu direct shear results for AP 104/5

Depth (m)	Width (m)	Clay and silt (%) from PSD*	Bulk Density (Mg/m^3)	c (kPa)	ϕ (°)	q_{all} (kPa)
5.20	1	43.8%	1.790	12.3	21	342
10.40	1	63.2%	1.745	18.5	15	348

Note:
* PSD = Particle size distribution or soil grading
ϕ = Internal angle of soil friction in degrees
q_{all} = Foundation's allowable bearing capacity
c = Cohesion of the soil

3.8 The One-Dimensional Consolidation Testing

The consolidation C_v value of 0.0042 cm^2/s in the range of 0.00032 to 0.0032 cm^2/s corresponded to a medium consolidation category, typical of 15-25% clays of the low plastic clay (CL) as per USCS system; whereas, the m_v values of 0.187 m^2/MN in the range of 0.25-0.125 (Table 15) and 0.1-0.3 (Table 16), corresponded to stiff or firm clays of consolidated lake deposits or lacustrine/swampy soils of medium compressibility properties of 0.05 to 0.15 compression index (C_c) [63,69].

Table 13: Insitu consolidation results for AP 104/5

Test Depth (m)	e_o (-)	γ_b (Mg/m^3)	c_v (cm^2/s)	m_v (m^2/MN)	p_o (kPa)
10.4 - 10.7	0.752	1.745	0.0042	0.187	201

Where:
e_o = Initial void ratio; γ_b = Initial bulk density;
c_v = Coefficient of consolidation
m_v = Coefficient of volume compressibility;
p_o = Pre-consolidation pressure

Table 14: Coefficient of consolidation

C_v Range cm^2/s	Category	Typical material	Soil classification (USCS)
< 0.000032	Very Low	-	-
0.000032 to 0.00032	Low	>25% Clay	Medium plasticity clays (CL-CH), and volcanic silt (MH)
0.00032 to 0.0032	Medium	15-25% Clay	Low plasticity clay/mud (CL)
0.0032 to 0.032	High	<15% Silt	Organic silt (OL)
> 0.032	Very High	-	-

C_v Range cm^2/s	Category	Typical material	Soil classification (USCS)

Note:
1 m^2/year = 5/15768 cm^2/s; C_v = coefficient of consolidation
Source: George et al. (2006), and Carter and Bentley (2016) [Adapted from Holtz and Kovacs (1981)]

Table 15: Coefficient of volume compressibility

m_v (m^2/MN)	Soil type
10.0 - 2.0	Peat
2.0 - 0.25	Plastic clay (normally consolidated alluvial clays)
0.25 - 0.125	Stiff clay
0.125 - 0.0625	Hard clay (boulder clays)

Note: m_v = Coefficient of volume compressibility
Source: Smith (2014)

Table 16: Compression index and descriptions

M_v m^2/MN	C_c	Category of compression	Soil Material Indicated
<0.05	0.025	Very Low compression	Hard over-consolidated glacial till, hard clay & stiff weathered rocks.
0.05 to 0.1	0.025 to 0.05	Low compression	Stiff glacial till/boulder clays, marls, very stiff tropical residual clays.
0.1 to 0.3	0.05 to 0.15	Medium compression	Firm clays of consolidated swampy or lake/ lacustrine deposits, glacial outwash clays, weathered marls, firm glacial till, normally consolidated clays at depth, firm tropical residual clays.
0.3 to 1.5	0.15 to 0.75	High compression	Poorly consolidated alluvial clays, estuarine deposits & sensitive clay
>1.5	0.75 to 5+	Very High compression	Highly organic alluvial clays, and peats.

Where:
C_c = compression index; m_v = coeff. of vol. compressibility; a_v = coefficient of compressibility

$$m_v = \left(\frac{a_v}{1+e_o}\right) = \left[\left(\frac{\delta_e}{\delta_p}\right) x \frac{1000}{(1+e_o)}\right]$$

Source: Carter & Bentley (2016) [Adapted from Bowles (1997)]

3.9 The Particle Size Distribution (Soil grading)

The particle size analysis showed that the soils at the formation levels of the locations AP 108/15 were poorly graded silty sand (SM), AP 108/20 were well graded clayey sand with gravel (SC), AP 104/5 were poorly graded clayey sand (SC) using the USCS classification system; whereas, the soils at KL 30 were gap graded gravelly clay (CI) as per the BS 5930 classification system. The gradations and soil classifications confirmed the previously inconclusive descriptions from the Test trial pit and borehole soil strata, parts of the preliminary soil consistency descriptions by DPL, specific gravity soil generalisations, material type identifications using the consolidation's m_v and C_v values, and the general soil type descriptions under plasticity index (PI) interpretations as discussed in sections 3.1, 3.2, 3.6, 3.8 and 3.10 respectively [58,61,63].

Table 17: Insitu soil grading summaries

Site	Soil Grading	Formation Level	Soil Classification
AP 108/15	Poorly-graded	2.75m	SM (USCS)
AP 108/20	Well-graded	3.50m	SC (USCS)
AP 104/5	Poorly-graded	~12.80m	SC (USCS)
KL 30	Gap-graded	4.50m	CI (BS 5930)

Note: USCS = Unified Soil Classification System;
BS 5930 = British Soil Classification System

3.10 The Plasticity Index Interpretations

The Atterberg tests showed that the soils at location AP 108/15 had PI values in range of 7-17, corresponding to medium-plastic soils of cohesive silty-sand type, whereas AP 108/20, KL 30 and AP 104/5 had soils with PI values greater than 17 (>17), corresponding to high plastic soils of cohesive clay type. Meanwhile, all the above locations had Liquid Limit (LL) values less than 50 (<50), corresponding to fine-grained soils with low swell potentials. The PI and LL test value interpretations were used in complementing the final classification and grading descriptions of the fine-grained soils as discussed in section 3.9 above [58,68].

Table 18: Insitu Atterberg limit summaries

Site	Atterberg Limits			FFL	PI value range
	LL	PL	PI	(m)	(From Table 19)
1 (PS)	24.7	12.5	12.20	2.75	7 - 17
2 (GS)	44.8	21.4	23.4	3.50	> 17
3 (WL)	38.4	16.6	21.8	4.50	> 17
4 (PL)	34.5	14.8	19.7	~12.80	> 17

Note:
1 = AP 108/15; 2 = AP 108/20; 3 = KL 30; 4 = AP 104/5; PS = Poor Soil; GS = Good Soil; WL = Waterlogged Location; PL = Pile Location; FFL = Foundation's Formation Level

Table 19: PI interpretations and cohesiveness

PI	Degree of Plasticity	Degree of Cohesiveness	Soil Type
0	Non-Plastic	Non-cohesive	Sand
< 7	Low Plastic	Partly cohesive	Silt
7-17	Medium Plastic	Cohesive	Silty-Sand
> 17	High Plastic	Cohesive	Clay

Source: Surendra and Sanjeev (2017)

Table 20: Atterberg Limits and Swell Potential

Liquid Limit (LL)	Plasticity Index (PI)	Swell Potential (SP)
< 50	< 25	Low
50 - 60	25 - 35	Marginal
> 60	> 35	High

Source: Pitts (1984); Kalantari (1991)

3.11 The Chemical Analysis Tests

The chemical tests were done as a conclusive test following the preliminary soil resistivity test in section 3.4 above, to determine the insitu pH, and presence of corrosion-causing sulphates and chlorides, in describing the insitu environmental exposure conditions as summarised in the Tables 21 and 22 below.

International Journal of Engineering Research & Technology (IJERT)
ISSN: 2278-0181
Vol. 8 Issue 11, November-2019

The SO_4 results showed that the soils at locations AP 108/15, AP 108/20 and AP 104/5 had values ≤ 3000 mg/kg (≤ 0.3% by weight) corresponding to XA1 exposure condition of slightly aggressive chemical environments; whereas, the KL 30 ground water had values of SO_4 > 600 ppm, corresponding to XA2 exposure condition of moderately aggressive chemical environment as shown in Tables 21 and 22 below.

The pH values for AP 108/15 and AP 108/20 were 5.38 and 5.22 respectively, corresponding to XA2 exposure condition of moderately aggressive chemical environment, whereas KL 30 and AP 104/5 had pH values of 6.27 and 6.10 respectively, corresponding to XA1 exposure condition of slightly aggressive chemical environments. Thus, the chemical analysis and pH conditions were reconciled to provide XA2 exposure conditions of moderately aggressive chemical environment for all locations as per BS EN 206 (2013).

Sulphate Resistant Cements (SRC) of strength class 42.5N and a 3.5% limited C_3A (chloro-aluminate) content were used under moderate water-cement ratios of 0.40 to 0.50 in order to inhibit the effects of chlorides forming insoluble chloro-aluminates (C_3A) upon combining with the Tricalcium Aluminate ($3CaO \cdot Al_2O_3$) in concrete.

Table 21: Insitu chemical test results

Site	${SO_4}^{2-}$ content (% by weight)	Cl^- content (g/l)	pH value	Sample type
1 (PS)	0.05% (500 ppm)	0.007 (7 ppm)	5.38	Soil
2 (GS)	0.06% (600 ppm)	0009 (9 ppm)	5.22	Soil
3 (WL)	0.0686% (686 ppm)	10 (10,000 ppm)	6.27	Ground water
4 (PL)	0	0.021 (21 ppm)	6.10	Soil

Where: 1 g/L = 1000 ppm; and 1 ppm = 1 mg/L = 0.001 g/L

Table 22: Measured SO_4 results interpretations

Site	Measured SO_4 (ppm)	Limiting values of SO_4 (ppm)*	Exposure condition*
1 (PS)	500	≥ 2000 and ≤ 3000 (soil)	XA1
2 (GS)	600	≥ 2000 and ≤ 3000 (soil)	XA1
3 (WL)	686	> 600 and ≤ 3000 (water)	XA2
4 (PL)	0	≥ 2000 and ≤ 3000 (soil)	XA1

NB: 1 = AP 108/15; 2 = AP 108/20; 3 = KL 30; 4 = AP 104/5; PS = Poor Soil; GS = Good Soil; WL = Waterlogged Location; PL = Pile Location
* **Source:** BS EN 203 (2013)

3.12 Concrete cube compressive strength Tests

The concrete cube compressive strength test was done as per BS EN 12390-1 (2012) and BS EN 12390-2 (2009), to determine the 7-day and 28-day strengths as a confirmatory quality control test of the 25 MPa design strength using 42.5N Sulphate Resistant Cement as shown in Table 23 below.
The results showed that all the locations had 7-day test strength values within the 104.2-123.36% range of the 25 MPa design value, and 28-day test strength values in the range of 155.12-211.08% of the 25 MPa design value. The compressive test values were used to confirm and provide assurance to the foundation's design concrete strength value of 25 MPa using 42.5N SRC as a remedy to the sulphate and chloride attacks, as discussed in section 3.11.

Table 23: Insitu compressive concrete cube results

Site	Tested Cube strength values [For a 28-day Design Strength (DS) of 25 MPa]			
	7-day strength		28-day strength	
	Results (MPa)	% of DS	Results (MPa)	% of DS
1 (PS)	29.81	119.24%	43.31	173.24%
2 (GS)	26.05	104.20%	38.78	155.12%
3 (WL)	27.71	110.84%	40.08	160.32%
4 (PL)	30.84	123.36%	52.77	211.08%

NB: 1 = AP 108/15; 2 = AP 108/20; 3 = KL 30; 4 = AP 104/5; PS = Poor Soil; GS = Good Soil; WL = Waterlogged Location; PL = Pile Location

3.13 Static Load Tests

The insitu static load tests were done to determine the insitu displacement and load capacity values of the foundations under tension/uplift, compression, and lateral load tests in conformity to IEC 61773 [57] as shown in Tables 24 to 26.
The static load test results showed that the location AP 104/5 exhibited maximum displacement values of 0.09 mm, -0.83 mm and 2.39 mm under tension, compression and lateral loading respectively; while locations AP 108/15, AP 108/20 and KL 30 exhibited maximum tension displacement values of 0.83 mm, 0.19 mm and 4.74 mm respectively. The limiting reference displacement values were 25 mm for both tension and compression loading tests, and 50 mm for the lateral loading test. The static load results were used in determining the slope (C_1) of the hyperbolic model graph's empirical line equation using Eq. (24) and (25) below, and in the calculation of the insitu foundation's load capacity (R_c) using Chin-Kondner extrapolation (1971) as per Eq. (26) below.

$$y = m\,x + c \quad \text{(Line of best fit)} \qquad (24)$$

$$\text{Slope} \Rightarrow C_1 = \frac{d}{dx}(y = m\,x + c) \qquad (25)$$

$$\text{Insitu Load Capacity} \Rightarrow \mathrm{R_c} = \frac{1}{\mathrm{C_1}} \ \text{(in kN)} \qquad (26)$$

The actual insitu load capacities of the test-foundations under static load methods were from 105.29% to 249.14% fraction of the prescriptive design values, which reaffirmed the conclusion that the load capacity results of the insitu-tested full-scale foundations exceeded the prescriptively designed load capacity values, as shown in Table 26.

Fig.1: Insitu static axial tension/uplift load test

Fig.2: Insitu static axial compression load test

Fig.3: Insitu static lateral load test

Table 24: Insitu static load test summaries

Site Location	Insitu Maximum Displacements (mm)			IEC 61773 (1996) Limit-value (mm)		
	T	C	L	T	C	L
AP 108/15	0.83	-	-	25	25	50
AP 108/20	0.19	-	-			
KL 30	4.74	-	-			
AP 104/5	0.09	-0.83	2.39			

Where:
T = Static Axial Tension/Uplift Loading Test
C = Static Axial Compression Loading Test
L = Static Lateral Loading Test

Table 25: Slope readings for insitu static load tests

Site Location	Graph Line Slopes (x 10^{-3})		
	Tension Test	Compression Test	Lateral Test
AP 108/15	0.9996	-	-
AP 108/20	1.3568	-	-
KL 30	0.8755	-	-
AP 104/5	0.7223	0.5019	5.2591

Table 26: Insitu foundation load capacities

Site	Load Capacities					
	Tension Test (kN)		Compression Test (kN)		Lateral Test (kN)	
	Insitu Load	UDL	Insitu Load	UDL	Insitu Load	UDL
1 (PS)	1000.4	945.36	-	-	-	-
2 (GS)	737.03	594.45	-	-	-	-
3 (WL)	1142.2	962.30	-	-	-	-
4 (PL)	1384.5	555.69	1992.43	1077.1	190.15	180.6

Note: 1 = AP 108/15; 2 = AP 108/20; 3 = KL 30; 4 = AP 104/5; PS = Poor Soil; GS = Good Soil; WL = Waterlogged Location; PL = Pile Location; UDL = Ultimate Design Load

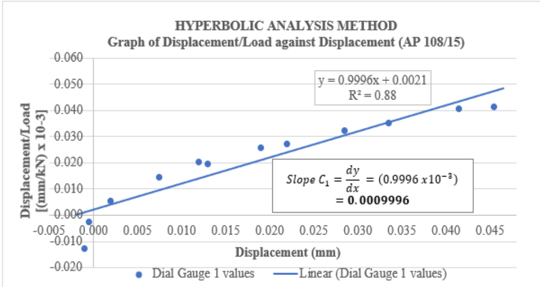

Fig.4: AP 108/15- Hyperbolic graph in uplift

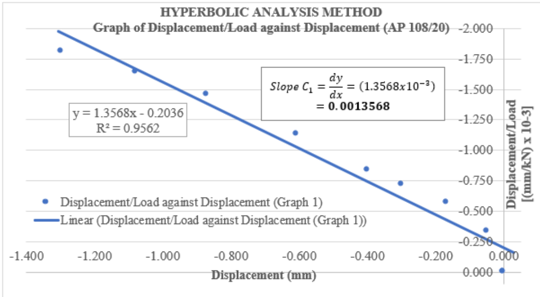

Fig.5: AP 108/20- Hyperbolic graph for uplift

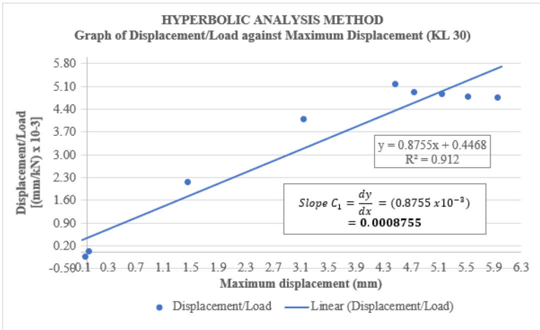

Fig.6: KL 30- Hyperbolic graph for uplift

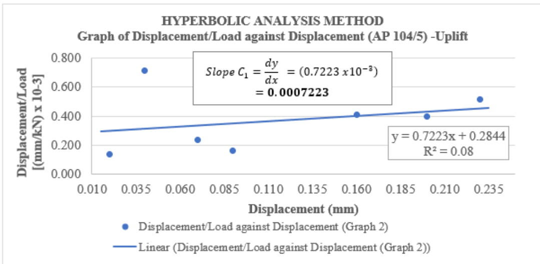

Fig.7: AP 104/5- Hyperbolic graph for uplift

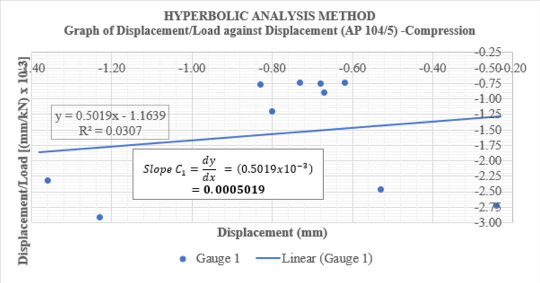

Fig.8: AP 104/5- Hyperbolic graph for compression

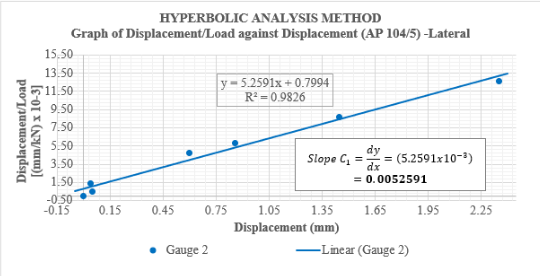

Fig.9: AP 104/5- Hyperbolic graph for lateral

4. CONCLUSION

Based on the reviews of the experimental results, the following conclusions were reached:

The insitu load capacities of the test foundations under static load were 105.29% to 249.14% fraction of the theoretical load capacities, confirming that the prescriptive design approaches use equations and methods governing a linear-elastic boundary in the design value extrapolations instead of the more-realistic plastic and non-linear approach.

The maximum insitu displacement values from static load tests differed significantly from that of the prescriptive design and technical specifications by being 0.36% to 18.96% fraction of the 25 mm prescriptive limit under uplift and 3.32% fraction of the prescriptive 25 mm under compression and 4.78% fraction of the prescriptive 50 mm limit under lateral test. These displacements were less than 19% of the prescriptive values as verified by the insitu static load tests of the foundations.

Due to the acidic soils and ground water, the use of 42.5N Sulphate Resistant Cement (SRC) led to very high compressive strength provided for the concrete foundations due to lack of a low grade 32.5N SRC in Uganda. This led to an overdesign in the concrete's compressive strength ranging from 104.2% to 123.36% of the design strength at 7 day and 155.12% to 211.08% at 28 days.

5. ACKNOWLEDGMENTS

The author would like to thank Sinohydro Corporation Ltd, Kalpataru Power Transmission Ltd, and GOPA-International Energy Consultants for their contributions towards the research at the Karuma Interconnection Project in Uganda.

6. REFERENCES

[1] Manjriker Gunaratne (2014) Foundation Engineering Handbook, 2nd Edition. ISBN-13: 978-14398-92787. CRC Press, Taylor & Francis, Florida, USA, pp 105 - 379.
[2] Kaushik C.P., Bhavikatti S.S. & Anubha Kaushik (2010) Basic Civil and Environmental Engineering. ISBN 13: 978-81-224-2850-6. New Age International (P) Ltd., New Delhi, India, pp 22 - 31.
[3] Sivakugan N. and Das, Braja M. (2011) Geotechnical Engineering- A Practical Problem-Solving Approach, ISBN-13: 978-1-60427-016-7. J. Ross Publishing, Inc., Florida, USA, pp 289 - 483.
[4] Federal Highway Administration (1992) Static Testing of Deep Foundations, Publication No. FHWA-SA-91-042. (Kyfor Z. G., Schnore A. R., Carlo T. A., and Baily P. F., eds), Soil Mechanics Bureau, NY State Department of Transportation, New York, USA, pp 1 - 165.
[5] Byrne, G. and Berry, A. (2008) A Guide to Practical Geotechnical Engineering in Southern Africa, 4th Edition. Franki Africa (Pty) Ltd, Cape Town, South Africa, pp 156 - 166.
[6] Monnet, Jacques (2015) In Situ Tests in Geotechnical Engineering. ISBN: 978-1-848-21849-9. ISTE Ltd, London, UK, pp 73 - 104.
[7] Cockerill, P., Nutter, J., Bradshaw, K., Ehrman, T., and Witney, J. (2017). East African Piling Limited Company Profile, March 2017, Available at: www.eastafricanpiling.com, Kampala, Uganda, pp 1 - 10.
[8] Tomlinson, M. J. and Boorman, R. (2001) Foundation Design and Construction, 7th Edn, ISBN: 0130-31180-4. Pearson Education, Essex CM20 2JE, England, pp. 1 - 547.
[9] Mosley Bill, John Bungey and Ray Hulse (2007) Reinforced Concrete Design to Eurocode 2, 6th Edition. ISBN-13: 9780230500716, Palgrave Macmillan Press, NY, USA, pp 15 - 308.
[10] Bayliss C.R. and Hardy B.J. (2011) Transmission and Distribution Electrical Engineering, 4th Edn, ISBN 978-0-08-096912-1. Elsevier Press, Oxford, UK, pp 615 - 629.
[11] Emuriat, Julius Emmanuel (2017) Parametric study on analysis and design of secant pile for earthquake loading, ISBN: 978-620-2-30082-7. Scholar's Press, Mauritius, pp 1 - 90.
[12] Przewłócki, J., Dardzińska, I. and Świniański, J. (2005) Review of historical buildings' foundations, Géotechnique, 55 (5), pp. 363 - 372. doi: 10.1680/geot.55.5.363.66017.
[13] Salgado, Rodrigo (2006) The engineering of foundations, 1st Ed. ISBN-13: 978-0072500585, McGraw-Hill, PA, USA, pp 21-896.
[14] An-Bin Huang and Hai-Sui Yu (2018) Foundation engineering Analysis and Design, 1st Edition, ISBN 13: 978-1-138-72079-4. CRS Press, Florida, USA, pp 189 - 239.
[15] Lacasse, S. and Nadim, F. (1994). Reliability issues and future challenges in geotechnical engineering for offshore structures. Proc., 7th Int. Conf. on Behaviour of Offshore Structures, Cambridge, Massachusetts, pp. 9 - 38.
[16] Gilbert, R. B. and Tang, W. H. (1995). "Model uncertainty in offshore geotechnical reliability." Proc. 27th Offshore Technology Conference, Houston, Texas, 557 - 567.
[17] Phoon, K. K and Kulhawy, F. H. (1999). Characterization of geotechnical variability. Canadian Geotechnical Journal, 36(4), 612 - 624.
[18] Whitman, R. V. (2000). Organizing and evaluating uncertainty in geotechnical engineering. Journal of Geotechnical and Geoenvironmental Eng., 126 (7), 583 - 593.
[19] Juang, C. H., Yang, S. H., Yuan, H., and Khor, E. H. (2004). Characterization of the uncertainty of the Robertson and Wride model for liquefaction potential evaluation. Soil Dynamics and Earthquake Engineering, 24(9), 771-780.
[20] Schuster, M.J., Juang, C. H., Roth, M.J.S., and Rosowsky, D. V. (2008). Reliability analysis of building serviceability problems caused by excavation. Géotechnique, 58(9), 743-749.
[21] Zhang, J., Zhang, L. M., and Tang, W. H. (2009). Bayesian framework for characterizing geotechnical model uncertainty. Journal of Geotechnical & Geoenvironmental Engineering, 135 (7), 932 - 940
[22] Juang, C. H., Fang, S. Y., Tang, W. H., Khor, E. H., Kung, G. T., and Zhang, J. (2009). Evaluating model uncertainty of an SPT-based simplified method for reliability analysis for probability of liquefaction. Soils and Foundations, 49 (12), 135 - 152.
[23] Zhang, J., Tang, W. H., Zhang, L. M., and Huang, H. W. (2012). Characterising geotechnical model uncertainty by hybrid Markov Chain Monte Carlo simulation. Computers and Geotechnics, 43, 26 - 36.
[24] Juang, C. H., Lei Wang, Sez Atamturktur, and Zhe Luo (2012). Reliability-based robust and optimal design of shallow foundations in

cohesionless soil in the face of uncertainty. Journal of GeoEngineering, Vol. 7, No. 3, pp. 075-087, doi: 10.6310/jog.2012.7 (3).1.

[25] Wu, T., Tang, W. H., Sangrey, D. A., and Baecher, G. B. (1989). Reliability of offshore foundations - state-of-the-art. Journal of Geotechnical Eng., 115 (2), 157 - 178.

[26] Christian, J. T., Ladd, C. C., and Baecher, G. B. (1994). "Reliability applied to slope stability analysis." Journal of Geotechnical Engineering, 120 (12), 2180 - 2207.

[27] Phoon, K. K., Kulhawy, F. H., and Grigoriu, M. D. (2003a). Development of a reliability-based design framework for transmission line structure foundations. Journal of Geotechnical and Geoenvironmental Eng, 129 (9), 798 - 806.

[28] Phoon, K. K., Kulhawy, F. H., and Grigoriu, M. D. (2003b). Multiple resistance factor design for shallow transmission line structure foundations. Journal of Geotechnical and Geoenvironmental Engineering, 129 (9), 807 - 818.

[29] Fenton, G. A., Griffiths, D. V., and Williams, M. B. (2005). Reliability of traditional retaining wall design. Géotechnique, 55 (1), 55-62.

[30] Najjar, S. and Gilbert, R. (2009). Importance of lower-bound capacities in the design of deep foundations. Journal of Geotechnical & Geoenvironmental Eng., 135 (7), 890 - 900.

[31] Wang, Y. (2011). Reliability-based design of spread foundations by Monte Carlo Simulations. Géotechnique, 61 (8), 677 - 685.

[32] Zhang, J., Zhang, L.M., and Tang, W.H. (2011). Reliability-based optimization of geotechnical systems. Journal of Geotechnical and Geoenvironmental Eng, 137 (12), 1211-1221.

[33] Venkatesh, K., Samadhiya, N. K. and Pandey, A. D. (2008). Approaches of analysis of ogee shaped barrage raft floor on varying foundation media. Proceedings of the 6th International Conf. on case histories in geotechnical eng. and symposium, Arlington, VA, August 11-16, 2008.

[34] Rodrigo Salgado et al. (2008) Analysis, Design, Testing and Performance of Foundations, Aug 11th -16th 2008, 6th International Conf. on Case Histories in Geotechnical Eng., pp. 1 - 23.

[35] Barvashov, V. A., Kharlamov, P. V., Naidenov, A. I. and Rytov, S. A. (2008). "Application of simplified models to qualitative geotechnical analysis" Proceedings of the 6th Intern. Conf. on case histories in geotechnical eng. and symposium, Arlington, VA, August 11-16, 2008.

[36] Murad Abu-Farsakh, Khalid Alshibli, and Anand Puppala (2017) Advances in analysis and design of deep foundations. Proceedings of the 1st GeoMEast International congress and exhibition, on sustainable civil infrastructures, ISBN 9783319616414, pp 1 - 300.

[37] Ministry of Energy and Mineral Development (2013) Technical Specifications for Karuma Hydropower Project and Associated Transmission Lines (MoE&MD, 2013)- Part A: Technical Specifications for Transmission Works, Republic of Uganda, pp. 1 - 260.

[38] Sriram, Kalaga and Prasad, Yenumula (2017) Design of electrical transmission line: structures and foundations, ISBN 9781315755687. CRC, London, UK, pp. 185-293.

[39] ASTM D2216-19 (2019) Standard test methods for laboratory determination of water (Moisture) content of soil and rock by mass, ASTM International, West Conshohocken, PA, 2019, www.astm.org

[40] ASTM D6913/D6913M-17 (2017) Standard test methods for particle-size distribution (Gradation) of soils using sieve analysis, ASTM International, West Conshohocken, PA, 2017, www.astm.org

[41] ASTM D2487-17 (2017) Standard practice for classification of soils for engineering purposes (Unified Soil Classification System), ASTM International, West Conshohocken, PA, 2017, www.astm.org

[42] ASTM D4318-17 (2017) Standard Test Methods for Liquid Limit, Plastic Limit, and Plasticity Index of Soils, ASTM International, West Conshohocken, PA, 2017, www.astm.org

[43] British Standards Institution (1990) BS 1377-2:1990. Methods of test for soils for civil engineering purposes. Classification tests. ISBN: 978-0 580 17867 6, London, BSI.

[44] British Standards Institution (1990) BS 1377-3:1990. Methods of test for soils for civil eng. purposes. Chemical and electro-chemical tests. ISBN 978058018370X, London, BSI.

[45] ASTM G51-18 (2018) Standard test method for measuring pH of Soil for use in corrosion testing, ASTM International, West Conshohocken, PA, 2018, www.astm.org

[46] ASTM D4327-11 (2011) Standard test method for anions in water by suppressed ion chromatography, ASTM International, West Conshohocken, PA, 2011, www.astm.org

[47] ASTM D7263-09 (2018) Standard test methods for laboratory determination of density (Unit Weight) of soil specimens, ASTM International, West Conshohocken, PA, 2018, www.astm.org

[48] ASTM D854-14 (2014) Standard test methods for specific gravity of soil solids by water pycnometer, ASTM International, West Conshohocken, PA, 2014, www.astm.org

[49] ASTM D3080/D3080M-11 (2011) Standard test method for direct shear test of soils under consolidated drained conditions, ASTM International, West Conshohocken, PA, 2011, www.astm.org

[50] British Standards Institution (1990) BS 1377-6:1990. Methods of test for soils for civil engineering purposes. Consolidation and permeability tests in hydraulic cells and with pore pressure measurement. ISBN 9780580 185885, London, BSI.

[51] ASTM D2435/D2435M-11 (2011) Standard test methods for one-dimensional consolidation properties of soils using incremental loading, ASTM International, West Conshohocken, PA, 2011, www.astm.org

[52] Tomlinson, M. J. and Woodward, J. (2015) Pile design and construction practice, 6th Edn, ISBN-13: 9781466592643. CRC Press, Taylor and Francis Group, Florida, USA, pp. 1 - 569.

[53] Hertlein, B. H., and Davis, A. G. (2006). Non-Destructive testing of Deep Foundations. ISBN 13: 9780470848500, John Wiley & Sons Ltd, West Sussex, England, pp 19 - 100.

[54] ASTM D1143/D1143M-07 (2013) e1, Standard test methods for deep foundations under static axial compressive load, ASTM International, West Conshohocken, PA, 2013, www.astm.org

[55] ASTM D3689/D3689M-07 (2013) e1, Standard test methods for deep foundations under static axial tensile load, ASTM International, West Conshohocken, PA, 2013, www.astm.org

[56] ASTM D3966/D3966M-07 (2013) e1, Standard test methods for deep foundations under lateral load, ASTM International, West Conshohocken, PA, 2013, www.astm.org

[57] IEC 61773 (1996) Overhead lines - Testing of foundations for structures, ASIN: B000XYS9YM, International Electrotechnical Commission, Geneva, Switzerland, www.iec.ch

[58] Das, Braja and Sobhan, Khaled (2018) Principles of Geotechnical Engineering. 9th Edn. Cengage Learning, Boston, USA, pp 710 - 742.

[59] British Standards Institution (2005) BS EN ISO 22476-2:2005+A1:2011. Geotechnical investigation and testing. Field testing. Dynamic probing. ISBN: 9780580749131, London, BSI.

[60] Nilsson, T. (2012). Parameter approach from DPL Nilsson Test, 3rd International Conf. on site characterisation, ISC-3, Taipei, Vol. 2, pp 1415-1418. Retrieved from www.nilsson.com.br

[61] Das, B. M. (2016) Principles of foundation engineering, 8th Edn. ISBN-13: 9781305081550. Cengage, Boston, USA, pp 1 - 911.

[62] Roberge, Pierre (2000) Handbook of corrosion engineering, 1st Edition, ISBN 9780070765160. McGraw-Hill, New York, USA, pp. 1 - 938.

[63] Smith, Ian (2014) Smith's element of soil mechanics, 9th Edition, ISBN 9780470673393. John Wiley & Son, West Sussex, UK, pp. 1- 459.

[64] Bowles, J. E. (1997). Foundation analysis and design, 5th Edition, ISBN 13: 9780079122476. McGraw-Hill, Singapore, pp 1 - 343.

[65] Tuncer, Erdil Riza, and Lohnes, R.A. (1977) An engineering classification for basalt-derived lateritic soils., Eng. Geol., 4, 319 - 339.

[66] Roy, Surendra and Dass, Gurcharan (2014) Statistical models for the prediction of shear strength parameters at Sirsa, India. ISSN 0976-4399, doi: 10.6088/ijcser.201404040002, International Journal of Civil and Structural Engineering, 4 (4), pp 483 - 498.

[67] Roy, Surendra, and Sanjeev Kumar Bhalla, (2017) Role of Geotechnical Properties of Soil on civil engineering structures, resources and environment, Vol. 7, No. 4, e-ISSN: 2163-2634, pp. 103-109. doi: 10.5923/j.re.20170704.0

[68] Das, B. M. (2019). Advanced soil mechanics. 5th Edn. ISBN-13: 9780815379133. CRC Press, Taylor & Francis, Florida, USA, pp 1 - 671.

[69] Carter, M., and Bentley, S. P. (2016) Soil properties and their correlation, 2nd Edition, ISBN: 978-1119130888. John Wiley and Sons Inc., West Sussex, UK, pg 1 - 217.